

Transform Domain Localized Processing Using Measured Steering Vectors and Non-Homogeneity Detection

Raviraj S. Adve*, Todd B. Hale, and Michael C. Wicks

Air Force Research Laboratory

Sensors Directorate/Radar Signal Processing Branch

Rome, NY, USA

Abstract— This paper presents two transform domain non-homogeneity detectors that account for the non-ideal array and the non-homogeneous interference environment. Each of these effects has been accounted for separately before [1,2]. However, this paper is the first attempt to incorporate both effects into a single STAP algorithm.

The formulation developed for the JDL algorithm is tested on measured data from the MCARM database. The example illustrates the effects in detection performance by considering both the non-ideal system and non-homogeneous interference scenario, individually and in combination. The results show that if only the non-homogeneous data is accounted for, the NHD might actually worsen the situation. Both system and interference scenario imperfections must therefore be accounted for.

INTRODUCTION

Space-Time Adaptive Processing (STAP) techniques promise to be the best means to suppress severe, dynamic, interference. Classical STAP algorithms achieve interference suppression through the use of the interference covariance matrix [3]. This covariance matrix is typically estimated using secondary data obtained from range cells close to the range cell under test, a technique termed symmetric windowing.

Statistical algorithms suffer when the secondary data does not reflect the statistics of the interference in the range cell of interest, a violation of the i.i.d. requirement. Such data is termed non-homogeneous. To quote [2], “A data set is termed wide sense homo-

geneous if the system performance loss can be ignored or is acceptable for a given STAP algorithm. A data set is said to be wide sense non-homogeneous if it is not wide sense homogeneous”.

Non-homogeneous data occurs in many practical situations such as airborne surveillance over land-sea interfaces, urban terrain, clutter discretely, etc. However, perhaps the most common non-homogeneity is the case of multiple targets at different ranges. Each target serves as a non-homogeneity resulting in a corrupted covariance matrix estimate and degraded detection performance.

To minimize the loss in performance due to non-homogeneous sample support, a Non-Homogeneity Detector (NHD) can be used to identify secondary data cells that do not reflect the statistical properties of the primary data [2, 4, 5]. These data samples are then excised from the covariance matrix estimate. Furthermore, the NHD can be used to rank order the secondary data cells in order of homogeneity. The samples deemed to be the most homogeneous are then used to form the covariance matrix estimate.

This paper focuses on NHDs used to improve the performance of the Joint Domain Localized (JDL) STAP algorithm [6]. The goal is to apply a NHD to improve the performance of the JDL algorithm. In this case, the measured data is obtained from the Multi-Channel Airborne Radar Measurements (MCARM) program [7]. The JDL algorithm is a post-Doppler beamspace approach that adaptively processes the radar data in the angle-Doppler domain. This paper uses the appropriate transform from the space domain to the angle domain based on measured steering vectors. The resultant spread in target infor-

*Dr. Adve is affiliated with Research Associates for Defense Conversion, Inc.

mation in the angle domain is accounted for by the formulation of [1].

The Generalized Inner Product (GIP) and JDL-MSMI (Modified Sample Matrix Inversion) tests are then used in the transform domain to detect non-homogeneities. While these two tests have been used to detect non-homogeneities in measured data [2], this approach has not been applied in conjunction with the formulation of [1]. The work of [2] therefore reflects the non-ideal scenario, but does not account for the non-ideal receiving system. This paper accounts for both realistic interference scenarios and realistic antenna arrays. The resulting improvement in STAP processing and target detection is significant.

THE JDL ALGORITHM USING MEASURED STEERING VECTORS

This effort focuses on the JDL algorithm [6] as extended to real antenna systems by Adev and Wicks [1]. This paper follows the formulation of [1], summarized here for completeness.

The first operation of the JDL algorithm transforms the raw space-time data to the angle-Doppler domain. The spatial steering vector associated with angle ϕ is the vector of voltages at the array due to a calibrated source at that angle. The appropriate transform from the space domain to the angle ϕ in the angle domain is an inner product of the spatial data with the corresponding conjugated steering vector. Similarly, the temporal steering vector associated with normalized Doppler $\bar{\omega}$ is the response of a single element due to a calibrated source offset from the carrier frequency by the corresponding Doppler frequency. The appropriate transform from the time domain to the point $\bar{\omega}$ in the Doppler domain is again an inner product with the corresponding conjugated steering vector.

In the case of an ideal linear array of equispaced, isotropic, point sensors, the spatial steering vector $\mathbf{a}(\phi)$ and the temporal steering vector $\mathbf{b}(\bar{\omega})$ can be written as

$$\mathbf{a} = \left[1 \ z_s \ z_s^2 \ \dots \ z_s^{(N-1)} \right]^T, \quad z_s = e^{j\frac{2\pi}{\lambda}d \sin \phi}, \quad (1)$$

$$\mathbf{b} = \left[1 \ z_t \ z_t^2 \ \dots \ z_t^{(M-1)} \right]^T, \quad z_t = e^{j2\pi\bar{\omega}}, \quad (2)$$

i.e. the spatial and temporal steering vectors form Fourier coefficients. Given an appropriate angle set, the conjugated spatial steering vectors become the columns of an N point DFT-matrix. Similarly, given an appropriate set of Doppler frequencies allows for the use of a M point DFT to transform the time domain data to the Doppler domain. The space-time data can therefore be transformed to the angle-Doppler domain using the two dimensional DFT

$$\tilde{\mathbf{X}} = \mathbf{W}_a^T \mathbf{X} \mathbf{W}_D, \quad (3)$$

where \mathbf{X} is the $N \times M$ data matrix with the N spatial returns for the m^{th} pulse in the m^{th} column. \mathbf{W}_a and \mathbf{W}_D are N point and M point DFT matrices respectively. $\tilde{\mathbf{X}}$ is the $N \times M$ angle-Doppler data for N angle and M Doppler frequencies.

The space-time steering vector is also transformed to the angle-Doppler domain using the transform given by Eqn. (3), i.e.

$$\tilde{\mathbf{S}} = \mathbf{W}_a^T \mathbf{S} \mathbf{W}_D, \quad (4)$$

$$\mathbf{S} = \mathbf{b}_t \otimes \mathbf{a}_t^T, \quad (5)$$

where \mathbf{a}_t and \mathbf{b}_t are the spatial and temporal steering vectors given by Eqns. (1) and (2) corresponding to the look angle ϕ_t and look Doppler $\bar{\omega}_t$. If the look angle and Doppler are chosen such that the conjugated spatial and temporal steering vectors form one of the columns of \mathbf{W}_a and \mathbf{W}_D respectively, then the matrix $\tilde{\mathbf{S}}$ has only one non-zero entry, i.e. the target information is localized to a single bin in angle-Doppler space. This results from the fact that the columns of a DFT matrix form an orthogonal set.

It is important to recognize that the DFT is the appropriate transform only for a very specific case. A 2-D DFT is valid only for an ideal linear array of equispaced isotropic sensors and if the angle-Doppler points are chosen to correspond to the DFT points. In any other case, the matrices \mathbf{W}_a and \mathbf{W}_D must be replaced with the matrices \mathbf{T}_a and \mathbf{T}_D whose columns are the conjugated steering vectors corresponding to the angles and Dopplers chosen, i.e.

$$\tilde{\mathbf{X}} = \mathbf{T}_a^T \mathbf{X} \mathbf{T}_D. \quad (6)$$

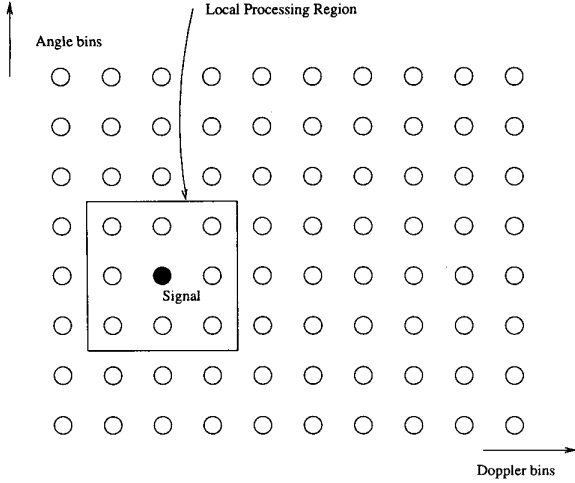


Fig. 1. LPR in JDL processing for an ideal array.

In the case of a real antenna such as the MCARM array, the columns of \mathbf{T}_a are the *measured* conjugated spatial steering vectors.

For a real array, the columns of \mathbf{T}_a are not orthogonal and hence the target information/steering vector is not confined to a single angle-Doppler bin. The spread of target information in angle-Doppler can be accounted for by also replacing \mathbf{W}_a in Eqn. (4) with \mathbf{T}_a , i.e. the space-time steering vector should be transformed to the angle-Doppler domain using *the same transformation as is used for the space-time data*. In prior work, researchers have transformed the data using Eqn. (6) and the steering vector using Eqn. (4) thereby neglecting the spread of the target in the angle domain [8]. The improvement in processing by accounting for target spread in the angle domain is illustrated in [1].

The transformation from space-time data to the angle-Doppler domain localizes the signal and the interference to a small region in the angle-Doppler domain. Adaptive processing is performed in a Localized Processing Region (LPR) centered around the signal as shown in Fig. 1. The size of the chosen LPR determines the adaptive DOF. The JDL algorithm is represented by the block diagram shown in Fig. 2.

The adaptive weight vector used within the LPR is given by

$$\mathbf{w}_{\text{LPR}} = \hat{\mathbf{R}}_{\text{LPR}}^{-1} \tilde{\mathbf{v}}, \quad (7)$$

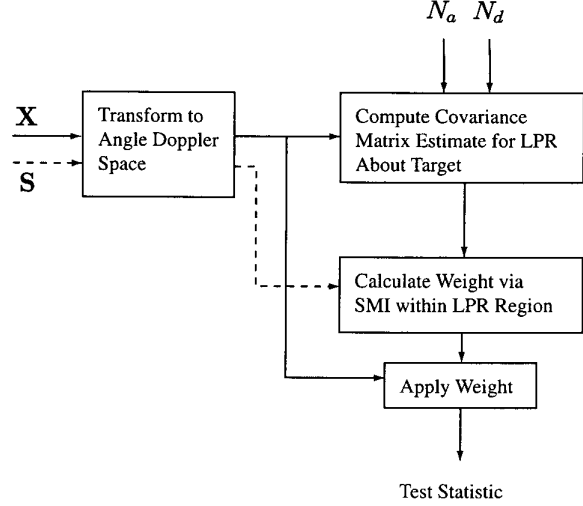


Fig. 2. Block diagram of the JDL algorithm.

where the angle-Doppler steering vector $\tilde{\mathbf{v}}$ is obtained by arranging the entries of $\tilde{\mathbf{S}}$ corresponding to the LPR in a vector. $\hat{\mathbf{R}}_{\text{LPR}}$ is the covariance matrix estimate corresponding to the LPR. This estimate is obtained using the secondary data after transformation to angle-Doppler space. The weight vector of Eqn. (7) is then applied to the primary data $\tilde{\chi}_{\text{LPR}}$ for the range cell of interest using the MSMI statistic [6] to obtain the output test statistic

$$\tilde{\eta}_{\text{JDL}} = \frac{|\mathbf{w}_{\text{LPR}}^H \tilde{\chi}_{\text{LPR}}|^2}{\tilde{\mathbf{v}}^H \hat{\mathbf{R}}_{\text{LPR}}^{-1} \tilde{\mathbf{v}}}. \quad (8)$$

TRANSFORM DOMAIN NON-HOMOGENEITY DETECTION

This paper applies two forms of non-homogeneity detection in conjunction with the JDL algorithm. The NHDs are the GIP [9, 10] and MSMI based detection [4, 5]. While other forms of NHDs are possible [2], these two NHDs have been most widely applied to measured data.

The GIP, also of the form of the Hotteling T^2 test, is based on using all available data, i.e. all K range cells to estimate a covariance matrix. The range cells are ranked according to the GIP statistic defined as

$$\eta_{\text{GIP}} = \tilde{\chi}^H \hat{\mathcal{R}}_K^{-1} \tilde{\chi}, \quad (9)$$

where $\hat{\mathcal{R}}_K$ is the covariance matrix estimated using all available data vectors from the K range cells in

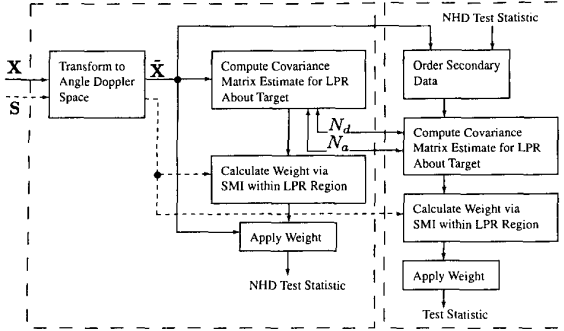


Fig. 3. Block diagram of the JDL-NHD method.

the LPR of the angle-Doppler domain. The outlying range cells (range cells with low or high GIP statistic) are deemed non-homogeneous and excised from the secondary data support. The GIP statistic in Eqn. (9) is the angle-Doppler counterpart to the space-time GIP statistic defined by Chen [9, 10]. Note that applying the GIP within the LPR results in a significant reduction in sample support required for the matrix inversion of $\hat{\mathcal{R}}_K$. The dimension of $\hat{\mathcal{R}}_K$ is determined by the size of the LPR, whereas in the space-time domain it is of dimension NM .

Chen [9, 10] has shown that GIP based non-homogeneity detection has many desirable properties. However, this formulation does not account for the STAP algorithm under consideration or the statistic being used for threshold comparison. For example, the GIP is independent of the steering vector and therefore look angle and Doppler. Hence, non-homogeneities with no significant impact on STAP processing for a particular look direction may be discarded. This is not judicious use of the limited secondary data supply.

The more efficient approach is to use the detection statistic as the NHD. With known covariance, i.e. the Matched Filter (MF) case, the detection statistic only contains thermal noise residue after STAP. Any significant deviations from the mean are caused by localized non-homogeneities such as discretions and targets. When the covariance is unknown and must be estimated, the range bins corresponding to these non-homogeneities contribute to covariance matrix estimation error.

TABLE I
RESULTS USING GIP AND JDL AS NHDs.

	JDL (dB)	JDL w/GIP NHD (dB)	JDL w/JDL NHD (dB)
Ignore Target Spread	4.6	2.7	5.7
Account for Target Spread	6.4	9.8	9.1

For these reasons, this work implements a first stage of JDL processing identical to the block diagram shown in Fig. 2, for the NHD. The JDL-MSMI output statistic for each range cell is then ranked according to magnitude and the data deemed most homogeneous is used to form a covariance matrix for the second stage of JDL processing. Figure 3 illustrates the proposed architecture.

NUMERICAL EXAMPLE

In this section, we present an example to illustrate the effects in detection performance by considering both the non-ideal system and non-homogeneous interference scenario. The example uses data from the MCARM database, a vast collection of clutter and signal measurements collected by an airborne radar over many flights with multiple acquisitions on each flight [7]. Included with the database is a set of measured steering vectors. These steering vectors are used in [8] and also here to transform spatial data to the angle domain. However, this paper uses the formulation of [1] to account for the spread of target information in the angle domain. A DFT is the valid transform to obtain Doppler domain information from the time domain data. The CPI uses 22 subarrays ($N=22$) to form a 2×11 rectangular array and 128 pulses ($M=128$).

The example presents results of the four possible cases: assuming ideal system and homogeneous data, assuming ideal system and accounting for non-homogeneous data, account for the non-ideal system and assuming homogeneous data and finally account-

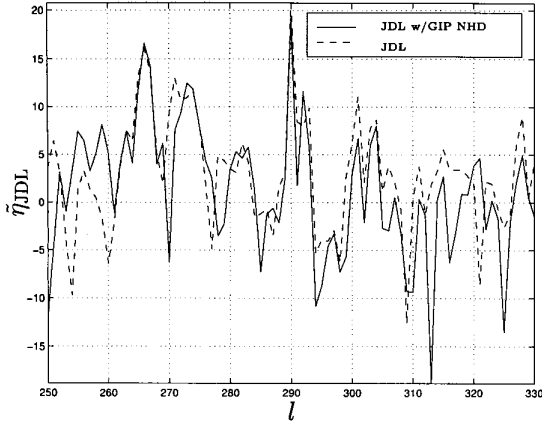


Fig. 4. The output of JDL algorithm with and without the GIP NHD, without accounting for target spread.

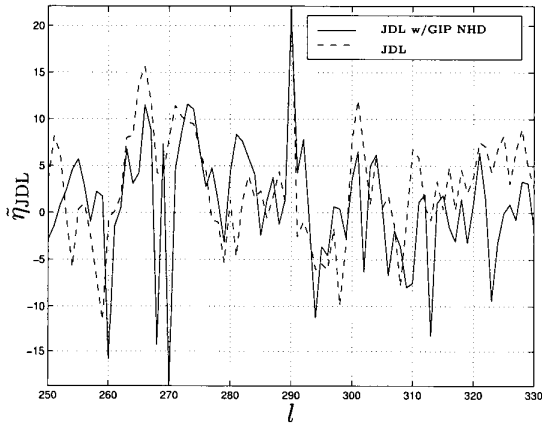


Fig. 5. The output of JDL algorithm with and without the GIP NHD, accounting for target spread.

ing for both non-ideal system and non-homogeneous data. For each case, the GIP and the JDL based NHD are considered.

A synthetic target of fixed amplitude, direction, Doppler, and range is injected into the MCARM data set. The amplitude and phase variation of the injected target across the 22 channels is obtained from the measured steering vectors. The amplitude of the injected target is chosen such that it remains undetected by non-adaptive digital beamforming/Doppler processing. In this example, the data from acquisition 575 on flight 5 is used. The parameters of the injected target are: Amplitude = 0.00005, Angle bin = 65 (Broadside), Doppler bin = -9 (-139.5Hz), and

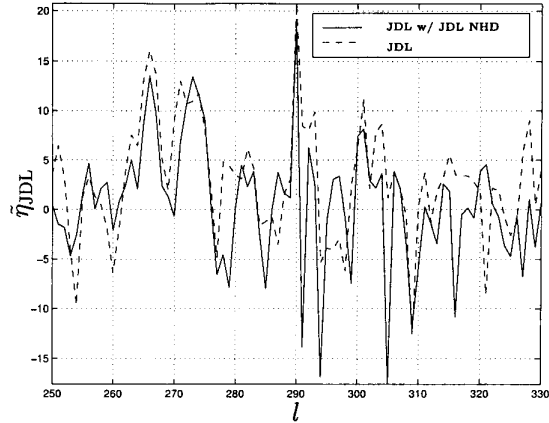


Fig. 6. The output of JDL algorithm with and without the JDL NHD, without accounting for target spread.

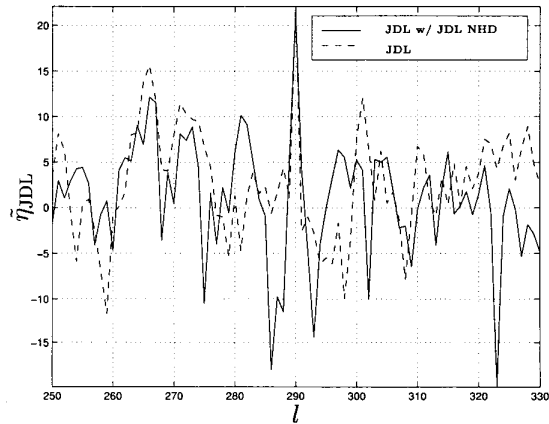


Fig. 7. The output of JDL algorithm with and without the JDL NHD, accounting for target spread.

Range bin = 290 .

JDL processing is performed at the target angle bin and for a few range bins surrounding the injected target. In this example, the figure of merit used to compare the two scenarios is the separation between the MSMI statistic at the target range/Doppler bin and the next highest statistic at other range or Doppler bins (the largest false alarm statistic). A large separation implies a large difference between target and residual interference, i.e. improving target detection while maintaining constant false alarm.

The results of the four cases considered above are presented in Figs. 4 and 5 for the GIP NHD and in Figs. 6 and 7 for the JDL NHD. Table I contains a

summary. The entries in the table are the separation between the peak at the range bin of the target and the next highest peak. The entries are hence a measure of detection performance.

The results show that in the case of applying JDL to measured data, certain non-homogeneity detectors may worsen the detection performance. The separation when applying JDL without accounting for target spread in angle is 4.6 dB. However, the separation decreases to 2.7 dB after using the GIP NHD. This situation is alleviated by accounting for the non-ideal array, i.e. the steering vector spreading in angle.

CONCLUSIONS

This paper presents two transform domain non-homogeneity detectors that account for the non-ideal array and the non-homogeneous interference environment. Each of these effects has been accounted for separately before [1, 2]. However, this paper is the first attempt to incorporate both effects into a single STAP algorithm.

The formulation developed for the JDL algorithm is tested on measured data from the MCARM database. The data includes clutter and noise. A target is injected using the measured steering vectors. The example illustrates the effects in detection performance by considering both the non-ideal system and non-homogeneous interference scenario, individually and in combination.

The results show that if only the non-homogeneous data is accounted for, the NHD might actually worsen the situation. Both system and interference scenario imperfections must be accounted for. The example shows significant improvements in STAP processing with as much as 5 dB improvement in the separation of the target statistic from the nearest false alarm.

REFERENCES

- [1] R. S. Adve and M. C. Wicks, "Joint domain localized processing using measured spatial steering vectors," in *Proceedings of the 1998 IEEE National Radar Conference*, May 1998.
- [2] H.-H. Chang, *Improving Space-Time Adaptive Processing (STAP) Radar Performance in Non-homogeneous Clutter*. PhD thesis, Division of Electrical Engineering and Computer Science, Syracuse University, Aug. 1997.
- [3] I. S. Reed, J. Mallett, and L. Brennan, "Rapid convergence rate in adaptive arrays," *IEEE Transactions on Aerospace and Electronic Systems*, vol. AES-10, No. 6, pp. 853–863, Nov. 1974.
- [4] M. C. Wicks, W. L. Melvin, and P. Chen, "An efficient architecture for nonhomogeneity detection in space-time adaptive processing airborne early warning radar," in *Proceedings of the 1997 International Radar Conference*, October 1997. Edinburgh, UK.
- [5] W. L. Melvin and M. C. Wicks, "Improving practical space-time adaptive radar," in *Proceedings of the 1997 IEEE National Radar Conference*, May 1997.
- [6] H. Wang and L. Cai, "On adaptive spatial-temporal processing for airborne surveillance radar systems," *IEEE Transactions on Aerospace and Electronic Systems*, vol. 30, pp. 660–669, July 1994.
- [7] D. Sloper, D. Fenner, J. Arntz, and E. Fogle, "Multi-channel airborne radar measurement (MCARM), MCARM flight test," Contract F30602-92-C-0161, Westinghouse Electronic Systems, Box 1693, Baltimore, MD 21203, Apr. 1996.
- [8] W. L. Melvin and B. Himed, "Comparitive analysis of space-time adaptive algorithms with measured airborne data," in *Proceedings of the 7th International Conference on Signal Processing Applications & Technology*, October 1996.
- [9] P. Chen, "On testing the equality of covariance matrices under singularity," contract, Rome Laboratory/OCSS, 26 Electronic Parkway, Rome, NY 13441-4514, Aug. 1994.
- [10] P. Chen, W. L. Melvin, and M. C. Wicks, "Partitioning procedure in radar signal processing problems," contract, Rome Laboratory/OCSS, 26 Electronic Parkway, Rome, NY 13441-4514, Aug. 1995.